Solving Monolithic Fluid-Structure Interaction Problems in Arbitrary Lagrangian Eulerian Coordinates with the deal.II Library

Thomas Wick
Institute of Applied Mathematics
University of Heidelberg, INF 293/294
69120 Heidelberg, Germany
E-mail: thomas.wick@iwr.uni-heidelberg.de

February 15, 2011

We briefly describe a setting of a non-linear fluid-structure interaction problem and its solution in the finite element software package deal.II. The fluid equations are transformed via the ALE map (Arbitrary Lagrangian Eulerian framework) to a reference configuration. The mapping is constructed using the biharmonic operator. The coupled problem is defined in a monolithic framework and serves for unsteady (or quasi-stationary) configurations. Different types of time stepping schemes are implemented. The non-linear system is solved by a Newton method. Here, the Jacobian matrix is build up by exact computation of the directional derivatives. The implementation serves for the computation of the fluid-structure benchmark configurations proposed by J. Hron and S. Turek.

Keywords: fluid-structure interaction, finite element method, monolithic, arbitrary Lagrangian Eulerian, implementation
2010 MSC: 35Q74, 35Q35, 65N30, 65M60, 68U20

1 Introduction

Fluid-structure interactions are of great importance in many real-life applications, such as industrial processes, aero-elasticity, and bio-mechanics. More specifically, fluid-structure interactions are important to measuring the flow around elastic structures, the flutter

analysis of airplanes [1], blood flow in the cardiovascular system, and the dynamics of heart valves (hemodynamics) [2, 3].

Typically, fluid and structure are given in different coordinate systems making a common solution approach challenging. Fluid flows are given in Eulerian coordinates whereas the structure is treated in a Lagrangian framework. We use a monolithic approach, where all equations are solved simultaneously. Here, the interface conditions, the continuity of velocity and the normal stresses, are automatically achieved. The coupling leads to additional nonlinear behavior of the overall system.

Using a monolithic formulation is motivated by upcoming investigations of gradient based optimization methods [4], and for rigorous goal oriented error estimation and mesh adaptation [5], where a coupled monolithic variational formulation is an inevitable prerequisite.

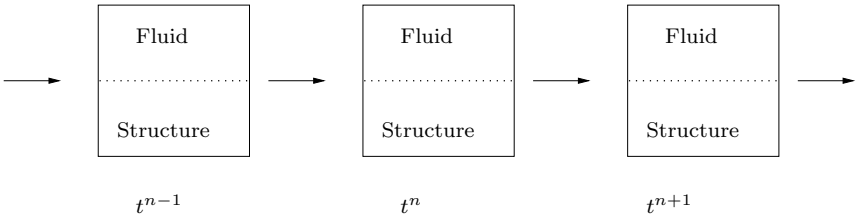

Figure 1: The monolithic solution approach for fluid-structure interaction

For fluid-structure interaction based on the 'arbitrary Lagrangian-Eulerian' framework (ALE), the choice of appropriate fluid mesh movement is important. In this work, we use the biharmonic operator (in a mixed formulation) for the mesh motion. It has the advantage to enable large deformations of the structure but has increased computational cost [6, 7].

Temporal discretization is based on finite differences and a formulation as one step-θ schemes [8], from which we can extract the implicit Euler, Crank-Nicolson, and the shifted Crank-Nicolson scheme.

Space discretization is done by using a standard Galerkin finite element approach. The solution of the discretized system can be achieved with a Newton method, which is very attractive because it provides robust and rapid convergence. The Jacobian matrix is derived by exact linearization which is demonstrated by an example. Because the development of iterative linear solvers is difficult for fully coupled problems (however, suggestions have been made [9, 10, 11]), we use a direct solver to solve the linear systems.

2 Equations in Variational Formulation

We denote by $\Omega \subset \mathbb{R}^d$, $d = 2, 3$, the domain of the fluid-structure interaction problem. This domain is supposed to be time independent but consists of two time dependent subdomains $\Omega_f(t)$ and $\Omega_s(t)$. The interface between both domain is denoted by $\Gamma_i(t) = \partial\Omega_f(t) \cap \partial\Omega_s(t)$. The initial (or later reference) domains are denoted by $\hat{\Omega}_f$ and $\hat{\Omega}_s$,

respectively, with the interface $\hat{\Gamma}_i$. Further, we denote the outer boundary with $\partial\hat{\Omega} = \hat{\Gamma} = \hat{\Gamma}_D \cup \hat{\Gamma}_N$ where $\hat{\Gamma}_D$ and $\hat{\Gamma}_N$ denote Dirichlet and Neumann boundaries, respectively.

We adopt standard notation for the usual Lebesgue and Sobolev spaces and their extensions by means of the Bochner integral for time dependent problems [12]. We use the notation $(\cdot,\cdot)_X$ for a scalar product on a Hilbert space X and $\langle\cdot,\cdot\rangle_{\partial X}$ for the scalar product on the boundary ∂X. For the time dependent functions on a time interval I, the Sobolev spaces are defined by $\mathcal{X} := L^2(I;X)$. Concretely, we use $\mathcal{L} := L^2(I;L^2(\Omega))$ and $\mathcal{V} := H^1(I;H^1(\Omega)) = \{v \in L^2(I;H^1(\Omega)) : \partial_t v \in L^2(I;H^1(\Omega))\}$.

2.1 Continuous level

In this section, we state a monolithic description of the coupled problem [7]. A continuous variable $\hat{u}$ in $\hat{\Omega}$, defining the deformation in $\hat{\Omega}_s$, and supporting the transformation in $\hat{\Omega}_f$ is defined. Then, we get the standard relations

$$\hat{\mathcal{A}} := \mathrm{id} + \hat{u}, \quad \hat{F} := I + \hat{\nabla}\hat{u}, \quad \hat{J} := \det(\hat{F}). \tag{1}$$

The ALE map is constructed by solving a mixed formulation of the biharmonic equation

$$\hat{\Delta}^2\hat{u} = 0 \quad \text{in } \hat{\Omega}, \tag{2}$$

in the sense of Ciarlet [13]. We introduce an auxiliary variable $\hat{w} = -\hat{\Delta}\hat{u}$ obtaining two differential equations:

$$\begin{aligned} \hat{w} &= -\hat{\Delta}\hat{u} \quad \text{in } \hat{\Omega}, \\ -\hat{\Delta}\hat{w} &= \quad 0 \qquad \text{in } \hat{\Omega}, \end{aligned} \tag{3}$$

with boundary conditions

$$\hat{u} = \hat{\partial}_n\hat{u} = 0 \quad \text{on } \hat{\Gamma}, \tag{4}$$

and the interface conditions:

$$\hat{u} = \hat{u}_s \quad \text{on } \hat{\Gamma}_i. \tag{5}$$

Moreover, in the case of the biharmonic mesh motion model, the first equation of (3) is defined on all $\hat{\Omega}$, whereas the second equation is only given in the fluid domain $\hat{\Omega}_f$.

Furthermore, the velocity $\hat{v}$ is a common continuous function for both subproblems, whereas the pressure $\hat{p}$ is discontinuous. We state the monolithic setting for fluid-structure interaction with a biharmonic mesh motion model:

Problem 2.1 (Variational fluid-structure interaction, biharmonic mesh motion)**.** Find $\{\hat{v}, \hat{u}, \hat{w}, \hat{p}\} \in \{\hat{v}^D + \hat{\mathcal{V}}^0\} \times \{\hat{u}^D + \hat{\mathcal{V}}^0\} \times \hat{\mathcal{V}} \times \hat{\mathcal{L}}$, such that $\hat{v}(0) = \hat{v}^0$ and $\hat{u}(0) = \hat{u}^0$, for almost all time steps t, and

$$\begin{aligned}
(\hat{J}\hat{\rho}_f \partial_t \hat{v}, \hat{\psi}^v)_{\hat{\Omega}_f} + (\hat{\rho}_f \hat{J}(\hat{F}^{-1}(\hat{v} - \partial_t \hat{u}) \cdot \hat{\nabla})\hat{v}), \hat{\psi}^v)_{\hat{\Omega}_f} \\
+(\hat{J}\hat{\sigma}_f \hat{F}^{-T}, \hat{\nabla}\hat{\psi}^v)_{\hat{\Omega}_f} + (\hat{\rho}_s \partial_t \hat{v}, \hat{\psi}^v)_{\Omega_s} + (\hat{J}\hat{\sigma}_s \hat{F}^{-T}, \hat{\nabla}\hat{\psi}^v)_{\hat{\Omega}_s} \\
-\langle \hat{g}, \hat{\psi}^v \rangle_{\hat{\Gamma}_N} - (\hat{\rho}_f \hat{J}\hat{f}_f, \hat{\psi}^v)_{\hat{\Omega}_f} - (\hat{\rho}_s \hat{f}_s, \hat{\psi}^v)_{\hat{\Omega}_s} = 0 \quad \forall \hat{\psi}^v \in \hat{V}^0, \\
(\hat{\alpha}_u \hat{w}, \hat{\psi}^w) + (\hat{\alpha}_u \hat{\nabla}\hat{u}, \hat{\nabla}\hat{\psi}^w)_{\hat{\Omega}} - \langle \hat{\alpha}_u \hat{n}_f \hat{\nabla}\hat{u}, \hat{\psi}^w \rangle_{\hat{\Gamma}_i} = 0 \quad \forall \hat{\psi}^w \in \hat{V}, \\
(\partial_t \hat{u} - \hat{v}, \hat{\psi}^u)_{\hat{\Omega}_s} + (\hat{\alpha}_w \hat{\nabla}\hat{w}, \hat{\nabla}\hat{\psi}^u)_{\hat{\Omega}_f} - \langle \hat{\alpha}_w \hat{n}_f \hat{\nabla}\hat{w}, \hat{\psi}^u \rangle_{\hat{\Gamma}_i} = 0 \quad \forall \hat{\psi}^u \in \hat{V}^0, \\
(\widehat{\mathrm{div}}\,(\hat{J}\hat{F}^{-1}\hat{v}_f), \hat{\psi}^p)_{\hat{\Omega}_f} + (\hat{p}_s, \hat{\psi}^p)_{\hat{\Omega}_s} = 0 \quad \forall \hat{\psi}^p \in \hat{L},
\end{aligned}$$

with $\hat{\rho}_f$, $\hat{\rho}_s$, ν_f, μ_s, λ_s, $\hat{F}_s$, $\hat{J}_s$, and positive diffusion parameters $\hat{\alpha}_u$ and $\hat{\alpha}_w$. The stress tensors, $\hat{\sigma}_f$ and $\hat{\sigma}_s$, are defined as

$$\hat{\sigma}_f := -\hat{p}_f I + \hat{\rho}_f \nu_f (\hat{\nabla}\hat{v}_f \hat{F}^{-1} + \hat{F}^{-T}\hat{\nabla}\hat{v}_f^T), \tag{6}$$

$$\hat{\sigma}_s := \hat{J}^{-1}\hat{F}(\lambda_s(\mathrm{tr}\hat{E})I + 2\mu_s \hat{E})\hat{F}^T. \tag{7}$$

The viscosity and the density of the fluid are denoted by ν_f and $\hat{\rho}_f$, respectively. The function $\hat{g}$ represents Neumann boundary conditions for both physical boundaries (e.g., stress zero at outflow boundary), and normal stresses on $\hat{\Gamma}_i$. Later, this boundary represents the interface between the fluid and the structure. The structure is characterized by the density $\hat{\rho}_s$, the Lamé coefficients μ_s, λ_s. For the STVK material, the compressibility is related to the Poisson ratio ν_s ($\nu_s < \frac{1}{2}$). External volume forces are described by the term $\hat{f}_s$.

The Problem 2.1 is completed by an appropriate choice of the two coupling conditions on the interface. The continuity of velocity across $\hat{\Gamma}_i$ is strongly enforced by requiring one common continuous velocity field on the whole domain $\hat{\Omega}$. The continuity of normal stresses is given by

$$(\hat{J}\hat{\sigma}_s \hat{F}^{-T}\hat{n}_s, \psi^v)_{\hat{\Gamma}_i} = (\hat{J}\hat{\sigma}_f \hat{F}^{-T}\hat{n}_f, \psi^v)_{\hat{\Gamma}_i}. \tag{8}$$

By omitting this boundary integral jump over $\hat{\Gamma}_i$ the weak continuity of the normal stresses becomes an implicit condition of the fluid-structure interaction problem.

Remark 2.1. The boundary terms on $\hat{\Gamma}_i$ in the Problem 2.1 are necessary to prevent spurious feedback of the displacement variables $\hat{u}$ and $\hat{w}$. For more details on this, we refer to [14]. However, we performed numerical experiments to study the influence of these terms. It turned out that these terms can be neglected.

2.2 Discrete level

To compute a solution to Problem 2.1, we first define a semi-linear form $\hat{A}(\hat{U}_m)(\hat{\Psi})$ and corresponding right hand side $\hat{F}(\hat{\Psi})$ [7]. The temporal discretization is based on finite differences and the one step-θ schemes [8]. Spatial discretization is done by a standard Galerkin finite element discretization. For more details on these aspects, we refer to [7].

2.3 Linearization

Time and spatial discretization results for each single time step in a nonlinear quasi-stationary problem

$$\hat{A}(\hat{U}_m)(\hat{\Psi}) = \hat{F}(\hat{\Psi}) \quad \forall \hat{\Psi} \in \hat{X}_h^0,$$

which is solved by a Newton-like method. Given an initial guess U_m^0, find for $j = 0, 1, 2, \ldots$ the update $\hat{\delta}\hat{U}_m$ of the linear defect-correction problem

$$\hat{A}'(\hat{U}_m^j)(\hat{\delta}\hat{U}_m, \hat{\Psi}) = -\hat{A}(\hat{U}_m^j)(\hat{\Psi}) + \hat{F}(\hat{\Psi}), \tag{9}$$

$$U_m^{j+1} = U_m^j + \lambda \hat{\delta}\hat{U}_m. \tag{10}$$

Here, $\lambda \in (0, 1]$ is used as damping parameter for line search techniques. The directional derivative $\hat{A}'(\hat{U})(\hat{\delta}\hat{U}, \hat{\Psi})$ is defined by

$$\hat{A}'(\hat{U})(\hat{\delta}\hat{U}, \hat{\Psi}) := \lim_{\varepsilon \to 0} \frac{1}{\varepsilon} \left\{ \hat{A}(\hat{U} + \varepsilon \hat{\delta}\hat{U})(\hat{\Psi}) - \hat{A}(\hat{U})(\hat{\Psi}) \right\} \tag{11}$$

$$= \frac{d}{d\varepsilon} \hat{A}_h(\hat{U} + \varepsilon \hat{\delta}\hat{U})(\hat{\Psi}) \Big|_{\varepsilon=0}. \tag{12}$$

Implementation aspects

In this section, we present an example of one specific directional derivative that includes all of the necessary steps. Derivation of the other expressions is straight forward, but for the convenience of the reader, it is not shown here.

Let us consider a part of the fluid convection term in ALE coordinates. As part of a semi-linear form, it holds

$$\hat{A}_{\text{conv}}(\hat{U})(\hat{\Psi}) = (\hat{\rho}_f \hat{J}(\hat{F}^{-1}\hat{\partial}_t \hat{u} \cdot \hat{\nabla})\hat{v}), \hat{\psi}^v)_{\hat{\Omega}_f} = (\hat{\rho}_f \hat{\nabla}\hat{v}\, \hat{J}\hat{F}^{-1}\, \hat{\partial}_t \hat{u}, \hat{\psi}^v)_{\hat{\Omega}_f}.$$

In this case, the directional derivative $\hat{A}'_{\text{conv}}(\hat{U})(\hat{\delta}\hat{U}, \hat{\Psi})$ in the direction $\hat{\delta}\hat{U} = \{\delta\hat{v}, \delta\hat{u}, \delta\hat{p}\}$ is given by

$$\hat{A}'_{\text{conv}}(\hat{U})(\hat{\delta}\hat{U}, \hat{\Psi}) = \left(\hat{\nabla}\delta\hat{v}\, \hat{J}\hat{F}^{-1}\, \frac{\hat{u} - \hat{u}^{m-1}}{k}, \hat{\psi}^v \right) \tag{13}$$

$$+ \left(\hat{\nabla}\hat{v}\, (\hat{J}\hat{F}^{-1})'(\delta\hat{u})\, \frac{\hat{u} - \hat{u}^{m-1}}{k}, \hat{\psi}^v \right) \tag{14}$$

$$+ \left(\hat{\nabla}\hat{v}\, \hat{J}\hat{F}^{-1} \frac{\delta\hat{u}}{k}, \hat{\psi}^v \right). \tag{15}$$

In two dimensions the deformation matrix reads in explicit form:

$$\hat{F} = I + \hat{\nabla}\hat{u} = \begin{pmatrix} 1 + \hat{\partial}_1\hat{u}_1 & \hat{\partial}_2\hat{u}_1 \\ \hat{\partial}_1\hat{u}_2 & 1 + \hat{\partial}_2\hat{u}_2 \end{pmatrix},$$

which brings us to

$$\hat{J}\hat{F}^{-1} = \begin{pmatrix} 1 + \hat{\partial}_2\hat{u}_2 & -\hat{\partial}_2\hat{u}_1 \\ -\hat{\partial}_1\hat{u}_2 & 1 + \hat{\partial}_2\hat{u}_2 \end{pmatrix},$$

and its directional derivative in direction $\delta\hat{u} = (\delta\hat{u}_1, \delta\hat{u}_2)$:

$$(\hat{J}\hat{F}^{-1})'(\delta\hat{u}) = \begin{pmatrix} \hat{\partial}_2\delta\hat{u}_2 & -\hat{\partial}_2\delta\hat{u}_1 \\ -\hat{\partial}_1\delta\hat{u}_2 & \hat{\partial}_2\delta\hat{u}_2 \end{pmatrix}.$$

This expression is part of the second term shown in Equation (15). The remaining expressions for directional derivatives can be derived in an analogous way. For more details on computation of the directional derivatives on the interface, please refer to [15, 14].

3 Features of the Implementation in deal.II

The implementation is very similar to the construction of the tutorial steps in deal.II [16]. First, we start by definition of the terms needed to build up the ALE map. Next, the fluid terms are mapped to some arbitrary reference domain, so we define a namespace to do that.

In the two main classes terms for the boundary and initial values are defined. Second, the problem at hand itself is treated.

In the function

```
setup_system ()
```

we define fluid and structure parameters for a specific configuration [17], the number of time steps and the time stepping scheme, and a routine to read the grid. Finally, we define the system matrix and corresponding vectors to solve the system.

In the function

```
assemble_system_matrix ()
```

we perform the computation of the Jacobian matrix of the non-linear system.

In the function

```
assemble_system_rhs ()
```

we compute the residuum of the non-linear system, i.e., the right hand side.

Moreover, we set the initial boundary conditions for the problem at hand in

```
set_initial_bc (...)
```

In each Newton step, Dirichlet boundary conditions must be set to zero. Therefore, we find a second function

```
set_newton_bc ()
```

where we apply homogenous Dirichlet conditions to the Newton method.

In the next function,

```
solve ()
```

we solve the linear systems with a direct solver from UMFPACK.

The Newton iteration is performed in

```
newton_iteration (...)
```

This method also includes some nice features, like a simple line search routine and a condition that decides whether the matrix should be build or not.

The following function is similar to a lot of functions in the tutorial steps and manages the output of our results:

```
output_results (...)
```

We compute different quantities of interest (here, stresses acting on the interface between fluid and structure) with the following function:

```
compute_drag_lift_fsi_fluid_tensor()
```

Point values (deflections of the structure) are computed with

```
compute_point_value (...)
```

In the last function

```
run ()
```

the time stepping scheme, and all remaining routines to solve the problem, are performed.

Summary

The implementation shows that fluid-structure interaction problems can (relatively) easy derived with deal.II. We use a lot of tools provided by the package. Moreover, we present a Newton method that can be used to solve any systems of equations (not only FSI). In addition, the user may play around with three different time stepping schemes. Finally, by omitting the structure terms (this can simply be realized by setting all material ids equal to 0), the user gets immediately a pure fluid solver because the transformation $\hat{F}$ is the identity and $\hat{J} = 1$. Then, all equations reduce to the well-known Navier-Stokes equations.

4 Numerical results

We consider the numerical benchmark tests FSI 1, FSI 2 and FSI 3, which were proposed in [17]. The configuration is sketched in Figure 2. New results can be found in [18, 19, 20].

The first test case results in a stationary regime but is computed within a pseudo time stepping process with the implicit Euler scheme. The shifted Crank-Nicolson scheme (FSI 3) and the Fractional-Step-θ scheme (FSI 2) were used for time discretization with different time step sizes k. To keep the implementation easy, the latter time stepping scheme is not provided in the source code available to this work.

Configuration

The computational domain has length $L = 2.5m$ and height $H = 0.41m$. The circle center is positioned at $C = (0.2m, 0.2m)$ with radius $r = 0.05m$. The elastic beam has length $l = 0.35m$ and height $h = 0.02m$. The right lower end is positioned at $(0.6m, 0.19m)$, and the left end is attached to the circle.

Control points $A(t)$ (with $A(0) = (0.6, 0.2)$) are fixed at the trailing edge of the structure, measuring x- and y-deflections of the beam.

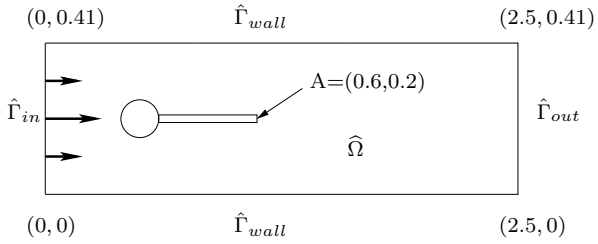

Figure 2: Flow around cylinder with elastic beam with circle-center $C = (0.2, 0.2)$ and radius $r = 0.05$.

Boundary conditions

A parabolic inflow velocity profile is given on $\hat{\Gamma}_{in}$ by

$$v_f(0,y) = 1.5\bar{U}\frac{4y(H-y)}{H^2}, \quad \bar{U} = 0.2ms^{-1} \quad \text{(FSI 1)},$$
$$v_f(0,y) = 1.5\bar{U}\frac{4y(H-y)}{H^2}, \quad \bar{U} = 1.0ms^{-1} \quad \text{(FSI 2)},$$
$$v_f(0,y) = 1.5\bar{U}\frac{4y(H-y)}{H^2}, \quad \bar{U} = 2.0ms^{-1} \quad \text{(FSI 3)}.$$

On the outlet $\hat{\Gamma}_{out}$ the 'do-nothing' outflow condition is imposed which leads to zero mean value of the pressure at this part of the boundary. The remaining boundary conditions are chosen as in the CSM test cases.

Initial conditions

For the non-steady tests one should start with a smooth increase of the velocity profile in time. We use

$$v_f(t;0,y) = \begin{cases} v_f(0,y)\frac{1-\cos(\frac{\pi}{2}t)}{2} & \text{if } t < 2.0s \\ v_f(0,y) & \text{otherwise.} \end{cases}$$

The term $v_f(0,y)$ is already explained above.

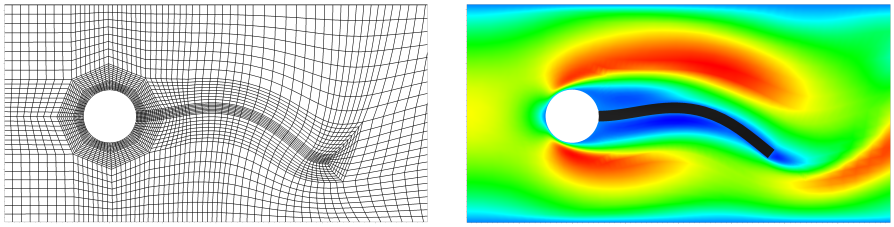

Figure 3: FSI 2 test case: mesh (left) and velocity profile in vertical direction (right) at time $t = 16.14s$.

Quantities of comparison and their evaluation

1) x- and y-deflection of the beam at $A(t)$.

2) The forces exerted by the fluid on the whole body, i.e., drag force F_D and lift force F_L on the rigid cylinder and the elastic beam. They form a closed path in which the forces can be computed with the help of line integration. The formula is evaluated on the fixed reference domain $\hat{\Omega}$ and reads:

$$(F_D, F_L) = \int_{\hat{S}} \hat{J}\hat{\sigma}_{all}\hat{F}^{-T} \cdot \hat{n}\, d\hat{s} \tag{16}$$

$$= \int_{\hat{S}(\text{circle})} \hat{J}\hat{\sigma}_f\hat{F}^{-T} \cdot \hat{n}_f\, d\hat{s} + \int_{\hat{S}(\text{beam})} \hat{J}\hat{\sigma}_f\hat{F}^{-T} \cdot \hat{n}_f\, d\hat{s}. \tag{17}$$

The quantities of interest for the time dependent test cases are represented by the mean value, amplitudes, and frequency of x- and y-deflections of the beam in one time period T of oscillations.

Parameters

We choose for our computation the following parameters. For the fluid we use $\varrho_f = 10^3 kgm^{-3}$, $\nu_f = 10^{-3}m^2s^{-1}$. The elastic structure is characterized by $\varrho_s = 10^4 kgm^{-3}$ (FSI 2) and $\varrho_s = 10^3 kgm^{-3}$ (FSI 1 and FSI 3), respectively, and $\nu_s = 0.4$. Further, we use for the FSI 1 and FSI 2 test cases $\mu_s = 0.5 * 10^6 kgm^{-1}s^{-2}$ and for the FSI 3 test case $\mu_s = 2.0 * 10^6 kgm^{-1}s^{-2}$.

The computed values are summarized in Tables 1 and 2. The results of the FSI 2 test are displayed in 4. The reference values are taken from [19]. In general, to verify convergence with respect to space and time, at least three different mesh levels and time step sizes should be presented.

Table 1: Results for the FSI 1 benchmark with the biharmonic mesh motion model. The mean value and amplitude are given for the four quantities of interest: $u_x, u_y[m], F_D, F_L[N]$.

DoFs	$u_x(A)[\times 10^{-5}]$	$u_y(A)[\times 10^{-4}]$	F_D	F_L
1914	2.3125	8.3715	13.9973	0.72215
7176	2.2674	8.6502	14.1162	0.76644
27744	2.2840	8.1227	14.2382	0.76460
109056	2.2746	8.1477	14.2713	0.76537
(ref.)	2.2700	8.2090	14.2940	0.76370

We observe the same qualitative behavior in each of our approaches for the quantities of interest ($u_x(A)$, $u_y(A)$, drag, and lift); these results are in agreement with [19].

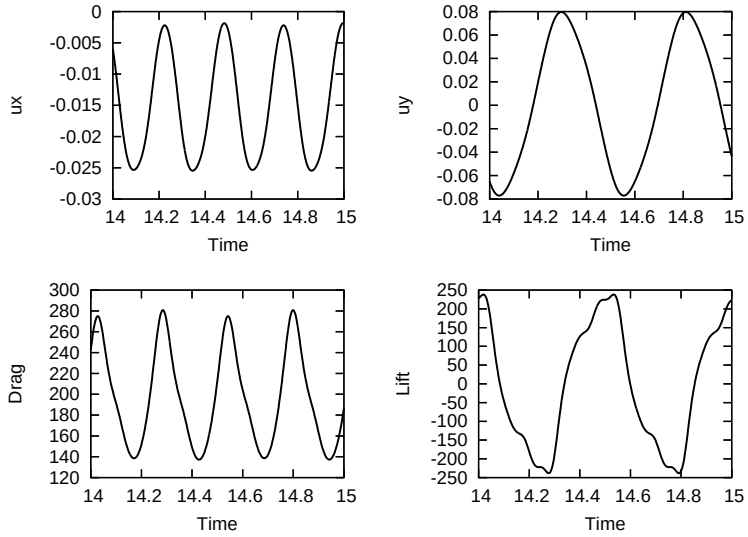

Figure 4: FSI 2. Top: deflections of the beam, $u_x(A)$ and $u_y(A)$. Bottom: drag and lift computations over the path S of the cylinder and the interface between fluid and structure.

5 How to Get the Source Code?

I am looking forward to sharing my source code with you. Please, feel free to write me an email

thomas.wick@iwr.uni-heidelberg.de

Because, I am really interested in new applications and results of fluid-structure interaction problems, I would like to ask you, to inform me when you create scientific papers with computations based on this source code,

6 Conclusions

We presented a description of an implementation of a fluid-structure interaction solver that is based on the deal.II library. In the future, we plan to add efficient mesh refinement procedures and gradient based optimization routines. For this kind of problems a closed monolithic formulation of the coupled problem, as presented in this work, is an indispensable requirement.

7 Acknowledgments

The author gratefully acknowledges Bärbel Janssen for proof reading this work.

Table 2: Results for the FSI 3 benchmark with the biharmonic mesh motion model. The mean value and amplitude are given for the four quantities of interest: $u_x, u_y[m], F_D, F_L[N]$. The frequencies $f_1[s^{-1}]$ and $f_2[s^{-1}]$ of u_x and u_y vary in a range of $10.53 - 10.84$ (ref. 10.93) and $5.37 - 5.44$ (ref. 5.46), respectively.

DoF	$k[s]$	$u_x(A)[\times 10^{-3}]$	$u_y(A)[\times 10^{-3}]$	F_D	F_L
7176	5.0e-3	-2.44 ± 2.32	1.02 ± 31.82	473.5 ± 56.97	8.08 ± 283.8
7176	2.0e-3	-2.48 ± 2.39	0.92 ± 32.81	471.3 ± 62.28	6.11 ± 298.6
7176	1.0e-3	-2.58 ± 2.49	0.94 ± 33.19	470.4 ± 64.02	4.65 ± 300.3
27744	5.0e-3	-2.43 ± 2.27	1.41 ± 31.73	483.7 ± 22.31	2.21 ± 149.0
27744	2.0e-3	-2.63 ± 2.61	1.46 ± 33.46	483.3 ± 24.48	2.08 ± 161.2
27744	1.0e-3	-2.80 ± 2.64	1.45 ± 34.12	483.0 ± 25.67	2.21 ± 165.3
42024	2.5e-3	-2.40 ± 2.26	1.39 ± 31.71	448.7 ± 21.16	1.84 ± 141.3
42024	1.0e-3	-2.53 ± 2.38	1.40 ± 32.49	449.7 ± 22.24	1.61 ± 142.8
42024	0.5e-3	-2.57 ± 2.42	1.42 ± 32.81	450.1 ± 22.49	1.49 ± 143.7
72696	2.5e-3	-2.64 ± 2.48	1.38 ± 33.25	451.1 ± 24.57	2.20 ± 150.4
72696	1.0e-3	-2.79 ± 2.62	1.28 ± 34.61	452.0 ± 25.78	1.91 ± 152.7
72696	0.5e-3	-2.84 ± 2.67	1.28 ± 34.61	452.4 ± 26.19	2.36 ± 152.7
(ref.)	0.25e-3	-2.88 ± 2.72	1.47 ± 34.99	460.5 ± 27.74	2.50 ± 153.91

References

[1] S. Piperno, C. Farhat, *Paritioned procedures for the transient solution of coupled aeroelastic problems - Part II: energy transfer analysis and three-dimensional applications*, Comput. Methods Appl. Mech. Engrg., 190 (2001) 3147–3170.

[2] C.A. Figueroa, I.E. Vignon-Clementel, K.E. Jansen, T.J.R. Hughes, C.A. Taylor, *A coupled momentum method for modeling blood ow in three-dimensional deformable arteries*, Comput. Methods Appl. Mech. Engrg. 195 (2006) 5685–5706.

[3] F. Nobile, C. Vergara, *An Effective Fluid-Structure Interaction Formulation for Vascular Dynamics by Generalized Robin Conditions*, SIAM J. Sci. Comput. , v.30 n.2 (2008) 731–763.

[4] R. Becker, H. Kapp, R. Rannacher, *Adaptive finite element methods for optimal control of partial differential equations: basic concepts*, SIAM J. Optim. Control 39, (2000) 113–132.

[5] R. Becker and R. Rannacher, *An optimal control approach to error control and mesh adaptation in finite element methods*, Acta Numerica 2001 (A. Iserles, ed.), Cambridge University Press (2001).

[6] B.T. Helenbrook, *Mesh deformation using the biharmonic operator*, Int. J. Numer. Meth. Engng. (2001) 1–30.

[7] T. Wick, *Fluid-Structure Interactions using Different Mesh Motion Techniques*, submitted revised version (2011).

[8] S. Turek, *Efficient solvers for incompressible flow problems*, Springer-Verlag, 1999.

[9] M. Heil, An efficient solver for the fully coupled solution of large-displacement fluid-structure interaction problems, *Comput. Methods Appl. Mech.*, 193, (2004) 1–23.

[10] S. Badia, A. Quaini, and A. Quarteroni, Splitting methods based on algebraic factorization for fluid-structure interaction, in *SIAM J. Sci. Comput.* 30(4), (2008) 1778–1805.

[11] T. Richter, A monolithic multigrid solver for 3d fluid-structure interaction problems, submitted, (2010).

[12] J. Wloka, *Partielle Differentialgleichungen*, B.G. Teubner, Stuttgart, 1987.

[13] P. G. Ciarlet, P.-A. Raviart, *A mixed finite element method for the biharmonic equation*, in Mathematical Aspects of Finite Elements in Partial Differential Equations (C.de Boor, Eds.), Academic Press, New York, 1974, pp. 125–145.

[14] T. Richter and T. Wick, *Finite Elements for Fluid-Structure Interaction in ALE and Fully Eulerian Coordinates,* Comput. Meth. Appl. Mech. Engrg. 199(41-44), (2010) 2633–2642.

[15] Th. Dunne, *Adaptive Finite Element Approximation of Fluid-Structure Interaction Based on Eulerian and Arbitrary Lagrangian-Eulerian Variational Formulations*, Dissertation, University of Heidelberg (2007).

[16] W. Bangerth and R. Hartmann and G. Kanschat, *Differential Equations Analysis Library*, Technical Reference. `http://www.dealii.org`

[17] J. Hron, S. Turek, *Proposal for numerical benchmarking of fluid-structure interaction between an elastic object and laminar incompressible flow*, in *Fluid-Structure Interaction: Modeling, Simulation, Optimization.* Lecture Notes in Computational Science and Engineering, Vol. 53, 146 - 170, Bungartz, Hans-Joachim; Schafer, Michael (Eds.), Springer, 2006.

[18] H.-J. Bungartz, M. Schäfer (Eds.), *Fluid-Structure Interaction: Modelling, Simulation, Optimization*, Springer Series: Lecture Notes in Computational Science and Engineering, Vol. 53, VIII, 2006.

[19] S. Turek, J. Hron, M. Madlik, M. Razzaq, H. Wobker, and J. F. Acker *Numerical simulation and benchmarking of a monolithic multigrid solver for fluid-structure interaction problems with application to hemodynamics*, Ergebnisberichte des Instituts für Angewandte Mathematik 403, Fakultät für Mathematik, TU Dortmund (2010).

[20] J. Degroote, R. Haelterman, S. Annerel, P. Bruggeman, J. Vierendeels, *Performance of partitioned procedures in fluid-structure interaction*, Comput. and Struct. 88 (2010) 446–457.